Latest issue   All issues   •••

Search in this journal

Nanotech Malaysia 2018, 7-9 May 2018, Universiti Teknologi Malaysia, Kuala Lumpur, Malaysia

⬇ Download full issue

‹ Previous vol/issue   Next vol/issue ›

Receive an update when the latest issues in this journal are published

🔔 Sign in to set up alerts

Research article ● Open access

Simulation of dielectrophoretic alignment for carbon nanotube on indium tin oxide

Abdullah Abdulhameed, Nurul Amziah Md Yunus, Izhal Abdul Halin, Mohd Nizar Hamidon
Pages 593-600

⬇ Download PDF   Article preview ⌄

Research article ○ Abstract only

Effect of processing temperature and foaming agent loading on properties of polylactic acid/kenaf fiber composite foam

Nur Adilah Abu Hassan, Sahrim Ahmad, Ruey Shan Chen, Farrah Diyana Zailan, Dalila Shahdan
Pages 601-606

⬇ Purchase PDF   Article preview ⌄

Research article ○ Abstract only

The effect of size of Au nanodisc on the localized surface plasmon resonance simulated using finite-difference time-domain (FDTD) method

Nor Ahya Hassan, Abdul Manaf Hashim
Pages 607-611

⬇ Purchase PDF   Article preview ⌄

Pages 668-674

Purchase PDF   Article preview ⌄

Research article ○ Abstract only

Effects of hydrogen during annealing process of graphene synthesis via chemical vapor deposition

Amir Hakimi Ramlan, Shukri Sirat, Edhuan Ismail, Yose Fachmi Buys, … Mohd. Hanafi Ani

Pages 675-685

Purchase PDF   Article preview ⌄

Research article ○ Abstract only

Structural, electronic and magnetic properties of Ca, Sr and Ba heterovalent A-site ion substitution in $BiFeO_3$ with different Fe oxidation states

Muhammad Haziq Ridzwan, Muhamad Kamil Yaakob, Mohamad Fariz Mohamad Taib, Ab Malik Marwan Ali, … Muhd Zu Azhan Yahya

Pages 686-691

Purchase PDF   Article preview ⌄

Research article ○ Abstract only

Characterization of Cr/Ag metal thin films interaction with infra-red laser

Aliyu Kabiru Isiyaku, Ahmad Hadi Ali, Noor Fauziyyah Ramly

Pages 692-696

Purchase PDF   Article preview ⌄

Research article ○ Abstract only

Photocatalytic degradation of aromatic organic pollutants: bulk versus mesoporous carbon nitride

Leny Yuliati, Shu Chin Lee, Hendrik O. Lintang

Pages 697-703

Purchase PDF   Article preview ⌄

Research article ○ Abstract only

Low temperature synthesis of silicon carbide nanowires on cathode for thermionic energy converter

Thye Jien Leong, Kamarul Aizat Abdul Khalid, Khairudin Mohamed

Pages 704-709

Purchase PDF   Article preview ⌄

Research article ○ Abstract only

Effect of post annealing treatment on electrical and structural properties of zinc oxide nanostructures

Muhammad Luqman Mohd Napi, Suhana Mohamed Sultan, Razali Ismail, Mohd Khairul Ahmad

Pages 710-714

Purchase PDF   Article preview ⌄

Research article ○ Abstract only

Atmospheric pressure plasma needle jet treated on aluminium thin film for semiconductor industries

Rizon Rizan Elfa, Nafarizal Nayan, Mohd Khairul Ahmad, Kusnanto Mukti Wibowo, … Ali Aldalbahi

Pages 715-720

Purchase PDF   Article preview ⌄

Research article ○ Abstract only

Citric acid cross-linking of highly porous carboxymethyl cellulose/poly(ethylene oxide) composite hydrogel films for controlled release applications

Nafeesa Mohd Kanafi, Norizah Abdul Rahman, Nurul Husna Rosdi

Pages 721-731

Research article ○ Abstract only

Influence of ultrathin chromium adhesion layer on different metal thicknesses of SPR-based sensor using FDTD

Najmiah Radiah Mohamad, Gan Siew Mei, Nur Akmar Jamil, BurhanuddinYeop Majlis, P. Susthitha Menon

Pages 732-737

Research article ○ Abstract only

Highly flexible and stretchable 3D graphene/MXene composite thin film

Nik Nurul Nazipah Ab Alim, Mohamed Salleh Mohamed Saheed, Norani Muti Mohamed, Mohamed Shuaib Mohamed Saheed

Pages 738-743

Research article ○ Abstract only

Properties of rapid thermal oxidized p-type germanium and its metal-oxide-semiconductor capacitor structure

Norani Ab Manaf, Abdul Manaf Hashim

Pages 744-753

Research article ○ Abstract only

Production of cellulose nano-crystals from bacterial fermentation

Norhayati Pa'e, Wen Ching Liew, Ida Idayu Muhamad

Pages 754-762

Research article ● Open access

Ultrasonic atomization of graphene derivatives for heat spreader thin film deposition on silicon substrate

Mohd Rofei Mat Hussin, Siti Aishah Mohamad Badaruddin, Nik Mohd Razali Mohd Nor, Mohd Hilmy Azuan Hamzah

Pages 763-769

Research article ○ Abstract only

Molecular structures of cooking palm oil in gas phase modelled by density functional theory

Saleha Maarof, Amgad Ahmed Ali, Abdul Manaf Hashim

Pages 770-775

Research article ○ Abstract only

Influence of surface energy and elastic strain energy on the graphene growth in chemical vapor deposition

Mohamad Shukri Sirat, Edhuan Ismail, Amir Hakimi Ramlan, Fatin Bazilah Fauzi, ... Mohd Hanafi Ani

Pages 776-783

Research article ○ Abstract only

Fe-assisted chemical bath deposition of highly oriented Cu_2O films and formation of ZnO nanorods/Cu_2O heterojunctions

Tomoaki Terasako, Ryutaroh Kitamoto, Hideyuki Okada

Pages 784-791

Research article ○ Abstract only

Piezoelectric energy harvester enhancement with graphene base layer

Lee Li Theng, Mohd Ambri Mohamed, Iskandar Yahya, Jothiramalingam Kulothungan, ... Hiroshi Mizuta

Pages 792-797

⬇ Purchase PDF   Article preview ⌄

Research article ○ Abstract only

Direct exfoliation of graphite and its Raman spectroscopic study

Nur Ubaidah Saidin, Kok Kuan Ying, Choo Thye Foo, Roshasnorlyza Hazan, Mahdi Ezwan Mahmoud

Pages 798-802

⬇ Purchase PDF   Article preview ⌄

Research article ○ Abstract only

Green sonochemical synthesis of gold nanoparticles using palm oil leaves extracts

Adamu Ibrahim Usman, Azlan Abdul Aziz, Osama Abu Noqta

Pages 803-807

⬇ Purchase PDF   Article preview ⌄

Research article ○ Abstract only

Improvement of Gas Barrier Properties of Polyethylene Terephtalate (PET) by Graphene Nanoplatelets (GNP)

Mohd Ihsan Che Mohd Noh, Mohd Ambri Mohamed, Ahmad Ghadafi Ismail, Mohd Hanafi Ani, Burhanuddin Yeop Majlis

Pages 808-815

⬇ Purchase PDF   Article preview ⌄

⟨ Previous vol/issue   Next vol/issue ⟩

Nanotech Malaysia 2018

Photocatalytic degradation of aromatic organic pollutants: bulk versus mesoporous carbon nitride

Leny Yuliati[a,*,b,c], Shu Chin Lee[d], Hendrik O. Lintang[a,b,c]

[a]Ma Chung Research Center for Photosynthetic Pigments, Universitas Ma Chung, Villa Puncak Tidar N-01, Malang 65151, East Java, Indonesia
[b]Department of Chemistry, Faculty of Science and Technology, Universitas Ma Chung, Villa Puncak Tidar N-01, Malang 65151, East Java, Indonesia
[c]Centre for Sustainable Nanomaterials, Ibnu Sina Institute for Scientific and Industrial Research, Universiti Teknologi Malaysia, 81310 UTM Johor Bahru, Johor, Malaysia
[d]Department of Chemistry, Faculty of Science, Universiti Teknologi Malaysia, 81310 UTM Johor Bahru, Johor, Malaysia

Abstract

Mesoporous carbon nitride (MCN) having larger specific surface area and more defects exhibited higher photocatalytic activity than the bulk one for degradation of aromatic organic pollutants under visible light. The different substituent groups resulted in the different degradation percentages. It was suggested that benzene derivatives with high structure stability or containing electron-withdrawing group (EWG) led to the deactivation of the aromatic ring. Although benzene ring reactivity was accelerated by the presence of electron-donating group (EDG), it was also affected by other factors such as the easiness to be adsorbed onto the photocatalyst and formation of no stable intermediates.

© 2018 Elsevier Ltd. All rights reserved.

Selection and peer-review under responsibility of the scientific committee of the Nanotech Malaysia 2018.

Keywords: carbon nitride; mesoporosity; defects; aromatic organic pollutants; electron-donating group; adsorption; intermediate

1. Introduction

Benzene derivatives are aromatic organic pollutants that can be easily found in industrial wastewater [1,2]. Their high stabilities in water might contaminate groundwater and will lead to adverse impact on the ecosystem. Therefore, an efficient waste water management is highly important. Semiconductor photocatalysis has been proposed as a good approach for environmental remediation [3-5]. It is a potential technology to treat wastewater as it can degrade

organic pollutants into non-toxic compounds. Among various semiconductor photocatalysts, titanium dioxide (TiO_2) is well-established for its good photocatalytic performance and has been extensively studied for the degradation of organic contaminants [3-6]. Furthermore, it is inexpensive and non-toxic. However, some problems still exist when TiO_2 is used for photocatalytic applications. For an example, TiO_2 possesses wide band gap energy (*Eg*) of *ca.* 3.2 eV, which can only be excited under UV light irradiation. Therefore, wide applications of TiO_2 using solar energy are limited since it can only be excited under UV light that comprise a small fraction of solar irradiation spectrum (5%). The possibility to use sunlight as the largest cost-free energy source in the Earth has motivated many researchers to develop visible light-driven photocatalysts, such as carbon nitride (CN).

Many studies on photocatalytic oxidation of benzene derivatives have been investigated on TiO_2. It has been reported that substituent groups on the aromatic ring (in terms of number and electronic nature) could affect the photocatalytic activity on the aromatic pollutants for formation of hydroxylated products [7,8] and photocatalytic degradation reaction [7-10]. Some papers claimed that the photocatalytic reactions of benzene derivatives (mono-, di-, and/or tri-substituted benzene) can be accelerated by the presence of electron-donating groups (EDG) that is activating and retarded by the presence of electron-withdrawing groups (EWG) that is deactivating [7,9,10]. However, there was also a report showing that reactivity of mono-substituted benzene was not much influenced by the electronic nature of substituent [8]. These findings suggested that there are other parameters influencing the aromatic ring reactivity. In this study, parameters leading to reactivity of benzene and its derivatives were investigated using bulk carbon nitride (BCN) and mesoporous carbon nitride (MCN) under visible light irradiation. Since aromatic ring reactivity could be complicated in the presence of more than one substituent, the benzene derivatives were limited to mono-substituted aromatic pollutants containing activating (toluene and phenol) or deactivating groups (benzoic acid), in order to reduce the possibility of combination effect coming from multiple substituent groups. As a comparison, non-substituted benzene and di-substituted pollutant containing both activating and deactivating groups (salicylic acid) were also studied. Some important parameters that affected the photocatalytic activity of the CN materials were also discussed from the point of views of both the nature of the aromatic organic pollutants and the photocatalyst properties.

2. Experimental

2.1. Synthesis of BCN and MCN

BCN was prepared through a simple thermal condensation reaction of urea precursor [11] in a ceramic crucible with cover under ambient pressure in air. Urea was grinded to powder (> 250 μm) before heating treatment in air at a rate of 2.2 K min^{-1} to 823 K for 4 h. The obtained yellow solid was then grinded to fine powder (150-250 μm) using porcelain mortar and pestle. The MCN was synthesized in a similar way to the reported MCN prepared from thermal polymerization of urea precursor [11] in the presence of nanocolloidal silica template with nanoparticles size of 7 nm. Initial mass ratio of urea to silica was fixed to 5 following the optimum photocatalytic activity reported in the literature [11]. The silica template was removed by ammonium hydrogen difluoride solution. After drying at 353 K in an oven overnight, the yellow solid was then grinded to fine powder (150-250 μm) using porcelain mortar and pestle.

2.2. Characterizations of BCN and MCN

The structural information such as chemical bonding on BCN and MCN samples was studied using Fourier transformed infrared (FTIR) spectrometer with a Thermo Scientific Nicolet iS50. The transmission spectra were collected using 32 scans at a resolution of 4 cm^{-1}. A standard potassium bromide (KBr) pellet technique was used in the measurements. Nitrogen adsorption-desorption analyses for BCN and MCN samples were measured at 77 K on a Micromeritics ASAP 2020 and BELSORP-Mini instrument, BEL Japan, respectively.

2.3. Photocatalytic testing over BCN and MCN

Prior to the photocatalytic reactions, adsorption of various aromatic organic pollutants in the presence of photocatalyst was conducted in dark condition. Typically, sample powder (50 mg) was added into a round bottom flask containing the aromatic organic pollutant solution (50 ppm in acetonitrile) with a water circulating system in order to minimize loss of volatile organic compounds. The mixture was then stirred in dark condition for several hours until adsorption-desorption equilibrium was achieved. Lastly, the powder sample was filtered out. The residue concentrations of benzene, benzoic acid, and salicylic acid were analyzed using a UV-Visible spectrophotometer (Perkin-Elmer Lambda 900), while the residue concentrations of toluene and phenol were analyzed using a GC-FID (Agilent 7820A).

The photocatalyst sample (50 mg) was dispersed in an open reactor system containing an organic pollutant (50 ppm, 50 mL). The mixture of photocatalyst and organic pollutant solution was then stirred for 1 h under dark condition to achieve adsorption equilibrium. A visible light source with a halogen fiber-optic illuminator equipped with an infrared cutoff filter (MI-150, 150 W, $\lambda > 400$ nm) was used to irradiate the reactor system for certain period of time (1-9 h) at room temperature. After separation of the sample, the filtrate was analyzed. The residue concentrations of benzene, benzoic acid, and salicylic acid were determined by the UV-Visible spectrophotometer, while the peak area of toluene and phenol were determined by the GC-FID. The percentage degradation of each aromatic organic pollutant was determined from the ratio of converted aromatic organic pollutant to the initial concentration.

3. Results and discussion

3.1. Properties of BCN and MCN

It has been reported that the BCN and MCN samples showed similar diffraction patterns, indicating that they possessed similar structure regardless the type of the precursor used in the synthesis [12,13]. However, reduced diffraction intensity was usually observed on the MCN due to the effect of the geometric confinement in the nanosized pore walls, which disturbed the ordered structure of CN. In order to clarify the difference on the structural property between the BCN and the MCN, characteristic chemical bonding of the BCN and MCN samples were studied by FTIR spectroscopy. Figure 1 depicts the FTIR spectra of both the BCN and MCN samples. All bands observed in the BCN were in the region of 810, 1200-1700, and 3000-3700 cm^{-1}, which were similar to those observed in the MCN. The presence of CN heterocycles was successfully shown by the vibration bands of both the samples in the region of 810 and 1200-1700 cm^{-1}. As compared to the BCN, an additional peak was observed at 2179 cm^{-1} for the MCN sample. This vibration band was attributed to C≡N or N=C=N group that is unfavourable for the formation of CN framework structure. This result suggested that the introduction of mesoporosity could break continuity of the CN network structure and led to not only a less condensed framework of the MCN, but also a less ordered structure as reported previously from their XRD patterns [12,13]. These bands were in good agreement with the previous reports of CN materials prepared via thermal polymerization reactions [14-16].
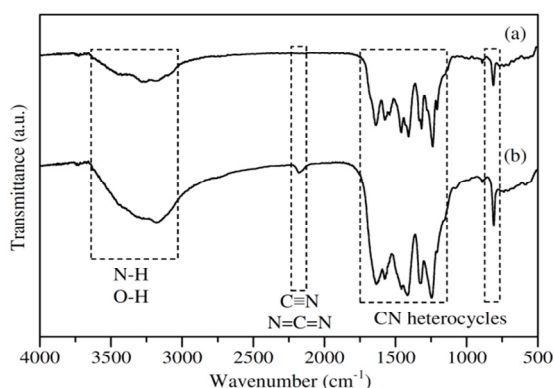

Fig. 1. FTIR spectra of (a) BCN and (b) MCN.

Figure 2 shows the nitrogen adsorption-desorption isotherms and BJH pore size distributions of the BCN and MCN samples. Both samples showed typical hysteresis loops of type IV isotherms with type H3 hysteresis loop corresponded to slit-shaped pores, suggesting the formation of mesoporous structure in these samples. It is worth noted here that even without involvement of template, the BCN showed the presence of mesopores. The BJH pore size of the BCN showed both small and large mesopores, with average pore sizes of *ca*. 3.7 and 18.4 nm, respectively (inset of Figure 2(a)). The obtained average pore values on the BCN were close to the reported BCN prepared from urea, showing average pores at *ca*. 3-5 nm and 18-28 nm [17,18]. The formation of porosity on the BCN could be caused by gases released such as NH_3 and H_2O during the thermal polymerization of urea precursor, which also has been reported elsewhere [17]. With the addition of 7 nm-silica template, a rather small quantity of bimodal mesopores of BCN at 3.7 and 18.4 nm were suppressed, but produced MCN with a relatively narrow pore distribution with an average mesopores at 7 nm (inset of Figure 2(b)). This finding suggested that silica template could tune the mesopores of CN and is important in preparing a uniform mesoporous material.

The BET specific surface area of the BCN and MCN were determined to be 38 and 191 m^2g^{-1}, respectively. The introduction of mesoporosity by the silica template contributed to the larger specific surface area on the MCN than the BCN. Although the BCN has smaller specific surface area than the MCN, the BCN showed larger specific surface area than other reported BCN samples prepared by cyanamide [15,19], dicyandiamide [14], and ammonium thiocyanate [14], which have specific surface area of 8-11, 8, and 9 m^2g^{-1}, respectively. Another group reported that the BCN prepared from urea possessed specific surface area of 70 m^2g^{-1}, which the value was *ca*. 6 times larger than the BCN prepared from other precursors, such as thiourea and dicyandiamide [17]. The larger specific surface area of the BCN prepared from urea than other precursors could be caused by the formation of porous structure due to release of gases (NH_3 and H_2O) during thermal condensation reaction of urea precursor.
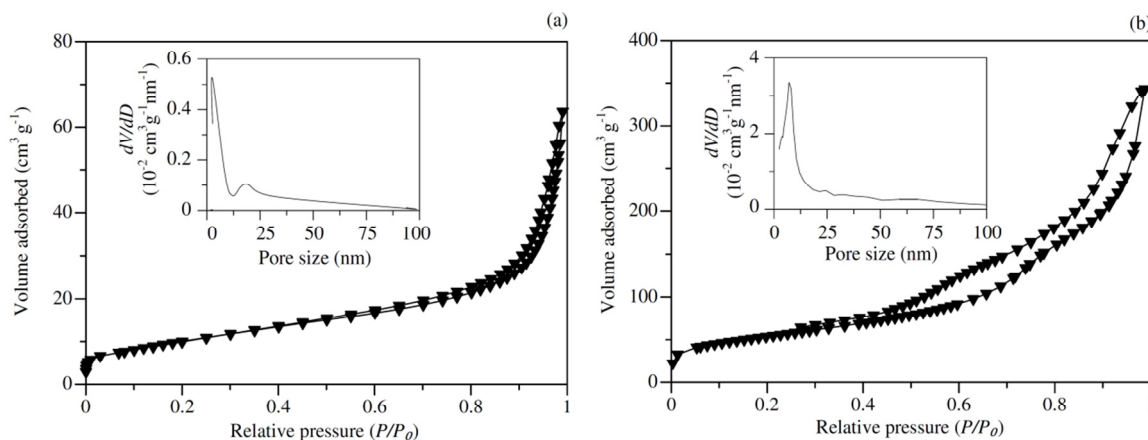

Fig. 2. Nitrogen adsorption-desorption isotherm of (a) BCN and (b) MCN. Insets show the pore size distribution.

3.2. Photocatalytic Activity of BCN and MCN

The photocatalytic activities of the BCN and MCN samples were tested for degradation of various aromatic organic pollutants including benzene, benzoic acid, toluene, phenol, and salicylic acid under visible light irradiation at various reaction times. Photolysis and adsorption experiments were also conducted. After visible light irradiation without photocatalyst, the concentrations of the aromatic benzene derivatives remained unchanged. This result indicated that the organic pollutants were stable under visible light and could not be degraded in the presence of visible light without photocatalyst. On the other hand, adsorption test for all types of benzene derivatives in the presence of photocatalyst under the dark condition showed that adsorption-desorption equilibrium was reached after 1 h. Adsorption of salicylic acid on the MCN was confirmed to be 10%. However, negligible amounts of adsorption by other benzene derivatives were obtained on BCN and MCN. All these results also confirmed that the organic pollutants could not be degraded in the presence of photocatalyst without visible light.

Table 1 summarizes the photocatalytic activities of the BCN and MCN samples for degradation of various aromatic organic pollutants after various reaction times. Under the same reaction time, although both of the BCN and MCN did not show photocatalytic activity for benzene (Entry 1) and benzoic acid (Entry 2), the MCN with larger specific surface area (191 m^2g^{-1}) showed better photocatalytic activity than BCN with smaller specific surface area (38 m^2g^{-1}) for the degradation of toluene (Entries 4 and 5), phenol (Entries 6-10), and salicylic acid (Entries 11-15). These results indicated that large specific surface area is one important property that can improve photocatalytic activity of CN photocatalyst. Larger specific surface area on MCN provides more exposed active sites for reaction to take place on the catalyst surface. The large specific surface area could increase number of photons absorbed, increasing formation of electron-hole pairs for the reaction of benzene derivatives to proceed, hence improved the photocatalytic activity of CN.

In addition to larger specific surface area, introduction of mesoporous structure onto CN also led to a less ordered structure on the MCN. The weakening of the *tris*-triazine network on MCN suggested the less formation of the N=C and terminal N-C groups in MCN, which might cause electron localization occurred easily on the surface sites (defects). Electron localization helps in reducing electrons-holes recombination [20], which could promote better photocatalytic activity on the MCN than the BCN. Another parameter for the good photocatalytic properties could be the better visible light absorption of the MCN than the BCN. Visible light trapping by the MCN due to light scattering of the mesoporous structure also could promote formation of electron-hole pairs for the degradation reaction of aromatic organic pollutants.

Table 1. Effects of substituents in the aromatic benzene derivatives on the photocatalytic degradation reactions on the BCN and MCN

Entry	Organic Pollutants	Substituent		Strength of EDG	Reaction time (h)	Degradation on BCN (%)	Degradation on MCN (%)
		EWG	EDG				
1	Benzene	-	-	-	9	0	0
2	Benzoic acid	-COOH	-	-	9	0	0
3					3	0	0
4	Toluene	-	-CH$_3$	Very weak	6	0	3
5					9	0	5
6					1	6	15
7					2	10	28
8	Phenol	-	-OH	Strong	3	13	39
9					6	34	76
10					9	56	97
11					1	3	12
12					2	7	27
13	Salicylic acid	-COOH	-OH	Strong	3	14	40
14					6	37	79
15					9	60	99

As shown in Table 1, the presence of different substituent groups in the benzene derivatives led to different photocatalytic activity, depending on the nature of substituent groups present in the aromatic system. As shown in Entry 1, the zero percentage of degradation for benzene was observed on the BCN and the MCN even after 9 h of visible light irradiation. No activity obtained would be due to the high stability of benzene, in good agreement with previous report [12]. The two equivalent resonance structures and closed shell of delocalized π electrons in the benzene aromatic ring lead to its high structure stability. Since the BCN and MCN did not show photocatalytic activity for benzene degradation, it is reasonable that the BCN and MCN also did not show activity for benzoic acid degradation during 9 h reaction due to the presence of carboxyl group as the deactivating EWG (Entry 2).

As for the aromatic benzene derivatives containing EDG, activity was observed on BCN and MCN for reaction time up to 9 h (Entries 3-20), except for the case of toluene degradation on BCN. As shown in Entries 3-5, toluene was not degraded on BCN even after 9 h of visible light reaction, while only low activity of 3 and 5% of toluene degradation was obtained for MCN after prolonged reaction time to 6 and 9 h, respectively. No or low activity obtained could be due to the fact that toluene has a methyl group that is a very weak EDG and therefore, has less benzene ring-activating property. Since methyl group is weakly activated, thus, it was reasonable that the degradation percentage of toluene was higher than benzene but lower than phenol and salicylic acid. In addition to the nature of the substituent, formation of stable intermediate was also one of the reasons for the low percentage degradation. Trace amount of benzaldehyde (less than 2 ppm) was detected by GC-FID after 6 and 9 h reaction. Formation of benzaldehyde as a by-product was also observed by another group when toluene was photocatalytically oxidized on TiO_2 in a non-aqueous medium in the presence of oxygen under UV irradiation for 2 h [21].

Salicylic acid and phenol were found to have similar reactivity to each other. As for phenol, with increasing reaction time from 1 to 9 h, the degradation percentage of phenol on both the BCN and MCN increased gradually (Entries 6-10), suggesting that the reaction occurred photocatalytically. After 9-h reaction time, 56% phenol was degraded on the BCN, while 97% was degraded on the MCN (Entry 10). The degradation was much higher than the one obtained for toluene (Entry 5), indicating the importance of hydroxyl group as the strong EDG that could activate the benzene ring. As for salicylic acid (Entries 11-15), it showed almost similar degradation to that of phenol (Entries 6-10) either on the BCN or MCN although it possesses both strong activating hydroxyl group and strong deactivating carboxyl group. In this case, the presence of the carboxyl group did not retard the aromatic ring reactivity. These results indicated that there is no significant effect from the carboxyl group of salicylic acid in benzene ring reactivity and other parameter might contribute to the high degradation of salicylic acid.

Another test conducted was the adsorption of the benzene derivatives on the MCN. Figure 3 shows the adsorption of benzene derivatives on the MCN after 1, 2, and 3 h. Salicylic acid was the only aromatic benzene derivative that showed 10% adsorption on the MCN, while adsorption of other aromatic organic pollutants on MCN was negligible. Better adsorption capability of salicylic acid on MCN as compared to other benzene derivatives suggested better interaction between the MCN and the salicylic acid molecules. Salicylic acid has two functional groups, which is a hydroxyl and a carboxyl group. Intermolecular hydrogen bonding might be formed between one functional group of salicylic acid and MCN, while another functional group of salicylic acid also might form such bonding with another salicylic acid molecule. Therefore, formation of two intermolecular hydrogen bondings on a salicylic acid molecule might improve adsorption capability of salicylic acid on MCN as compared to other mono-substituted benzene derivatives, leading to better interaction between MCN and salicylic acid. This might lead to the less effect of carboxyl group as the EWG in salicylic acid and resulted in the almost similar high photocatalytic activity to the degradation of phenol (Table 1, Entries 6-10 and 11-15). The importance of good adsorption of pollutants on photocatalyst for high photocatalytic activity was also reported by other research group, which salicylic acid was decomposed more rapidly than phenol due to its stronger adsorption on porous TiO_2 prepared by a sol-gel method [22]. The result suggested that the effect of adsorption capability of pollutant on catalyst surface is more dominant than the presence of deactivating carboxyl EWG for the high photocatalytic activity on the MCN.
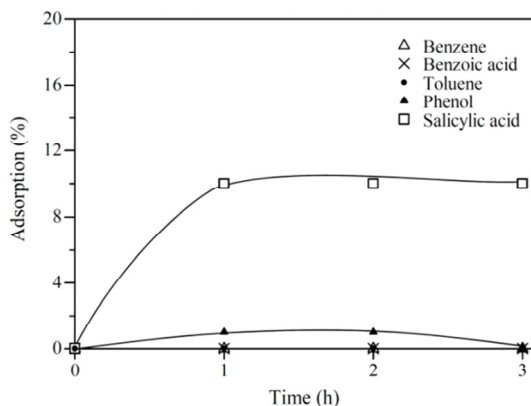

Fig. 3. Adsorption of various aromatic organic pollutants on MCN

4. Conclusions

BCN and MCN were successfully prepared by thermal polymerization of urea precursor. The characterization results showed that the generation of mesoporosity resulted in the larger specific surface area and the formation of defects. The CN samples were investigated for photocatalytic degradation of various aromatic organic pollutants under visible light irradiation. From the point of view of photocatalyst properties, larger specific surface area provided more exposed sites for reaction to occur on the MCN than the BCN, while defects formation might improve charge separation by trapping photoexcited electrons that could reduce electron-hole recombination, leading to higher activity on the MCN than the BCN. From the point of view of benzene derivatives properties, nature of substituents influenced reactivity of benzene ring. No photocatalytic activity was observed in the degradation of benzene and benzoic acid due to the high structure stability and ring deactivation by electron-withdrawing group (EWG), respectively. Low activity was obtained for toluene (5%) because it has a weak methyl electron-donating group (EDG) and induced formation of benzaldehyde intermediate. On the other hand, high percentage degradation was observed on phenol (97%) due to the presence of strong hydroxyl EDG. Salicylic acid having both EDG and EWG still could be removed easily (99%) due to the good adsorption of salicylic acid.

Acknowledgements

References

[1] G. Busca, S. Berardinelli, C. Resini, L. Arrighi, J. Hazard. Mater 160 (2008) 265–288.
[2] Q. Lan, L. Zhang, G. Li, R. Vermeulen, R.S. Weinberg, M. Dosemeci, S.M. Rappaport, M. Shen, B.P. Alter, Y. Wu, W. Kopp, S. Waidyanatha, C. Rabkin, W. Guo, S. Chanock, R.B. Hayes, M. Linet, S. Kim, S. Yin, N. Rothman, M.T. Smith, Science 306 (2004) 1774–1776.
[3] J.-M. Herrmann, Catal. Today 53 (1999) 115–129.
[4] M.R. Hoffmann, S.T. Martin, W. Choi, D.W. Bahnemann, Chem. Rev. 95 (1995) 69–96.
[5] R. Vinu, G. Madras, J. Indian Inst. Sci. 90 (2010) 189–230.
[6] M. Lazar, S. Varghese, S. Nair, Catalysts 2 (2012) 572–601.
[7] M.J. Sampaio, C.G., Silva, A.M.T. Silva, V.J.P. Vilar, R.A.R. Boaventura, J.L. Faria, Chem. Eng. J. 224 (2013) 32–38.
[8] C.G. Silva, J.L. Faria, Appl. Catal. B: Environ. 101 (2010) 81–89.
[9] S. Parra, J. Olivero, L. Pacheco, C. Pulgarin, Appl. Catal. B: Environ. 43 (2003) 293–301.
[10] C.G. Silva, J.L. Faria, ChemSusChem 3 (2010) 609–618.
[11] S.C. Lee, H. O. Lintang, L. Yuliati, Chem. Asian. J.7 (2012) 2139–2144.
[12] S.C. Lee, H. O. Lintang, S. Endud, L. Yuliati, Adv. Mater. Res. 925 (2014) 130–134.
[13] M.S. Sam, P. Tiong, H. O. Lintang, S. L. Lee, L. Yuliati, RSC Adv. 5 (2015) 44578–44586.
[14] Y. Cui, J. Zhang, G. Zhang, J. Huang, P. Liu, M. Antonietti, X. Wang, J. Mater. Chem. 21 (2011) 13032–13039.
[15] L. Yuliati, A.H.A. Kadir, S.L. Lee, H.O. Lintang, Malay. J. Anal. Sci. 21 (2017) 1342–1351.
[16] N.S. Alim, H.O. Lintang, L. Yuliati, J. Teknol. (Sci. & Eng.) 76 (2015) 1–6.
[17] Y. Zhang, J. Liu, G. Wu, W. Chen, Nanoscale 4 (2012) 5300–5303.
[18] F. Dong, Z. Wang, Y. Sun, W.-K. Ho, H. Zhang, J. Coll. Interf. Sci. 401 (2013) 70–79.
[19] X. Wang, K. Maeda, X. Chen, K. Takanabe, K. Domen, Y. Hou, X. Fu, M. Antonietti, J. Am. Chem. Soc. 131 (2009) 1680–1681.
[20] Y. Cui, J. Huang, X. Fu, X. Wang, Catal. Sci. Technol. 2 (2012) 1396–1402.
[21] M. Fujihira, Y. Satoh, T. Osa, J. Electroanal. Chem. Interf. Electrochem. 126 (1981) 277–281.
[22] K. Chhor, J.F. Bocquet, C. Colbeau-Justin, Mater. Chem. Phys. 86 (2004) 123–131.